

This is the peer reviewed version of the following article:

Identification of tumor-associated antigens with diagnostic ability of colorectal cancer by in-depth immunomic and seroproteomic analysis

María Garranzo-Asensio, Pablo San Segundo-Acosta, Carmen Povés , María Jesús Fernández-Aceñero, Javier Martínez-Useros, Ana Montero-Calle, Guillermo Solís-Fernández, Maricruz Sanchez-Martinez, Nuria Rodríguez, María Ángeles Cerón, Servando Fernandez-Diez, Gemma Domínguez, Vivian de Los Ríos, Alberto Peláez-García, Ana Guzmán-Aránguez, Rodrigo Barderas.

J Proteomics. 2020 Mar 1;214:103635.

which has been published in final form at

<https://doi.org/10.1016/j.jprot.2020.103635>

Manuscript Number: JPROT-D-19-00483R2

Title: Identification of tumor-associated antigens with diagnostic ability of colorectal cancer by in-depth immunomic and seroproteomic analysis

Article Type: Full Length Article

Section/Category: Original Article

Keywords: Colorectal cancer; immune response; Seroproteomics; Diagnostic autoantibody biomarkers; Mass spectrometry

Corresponding Author: Dr. Rodrigo Barderas, Chemistry

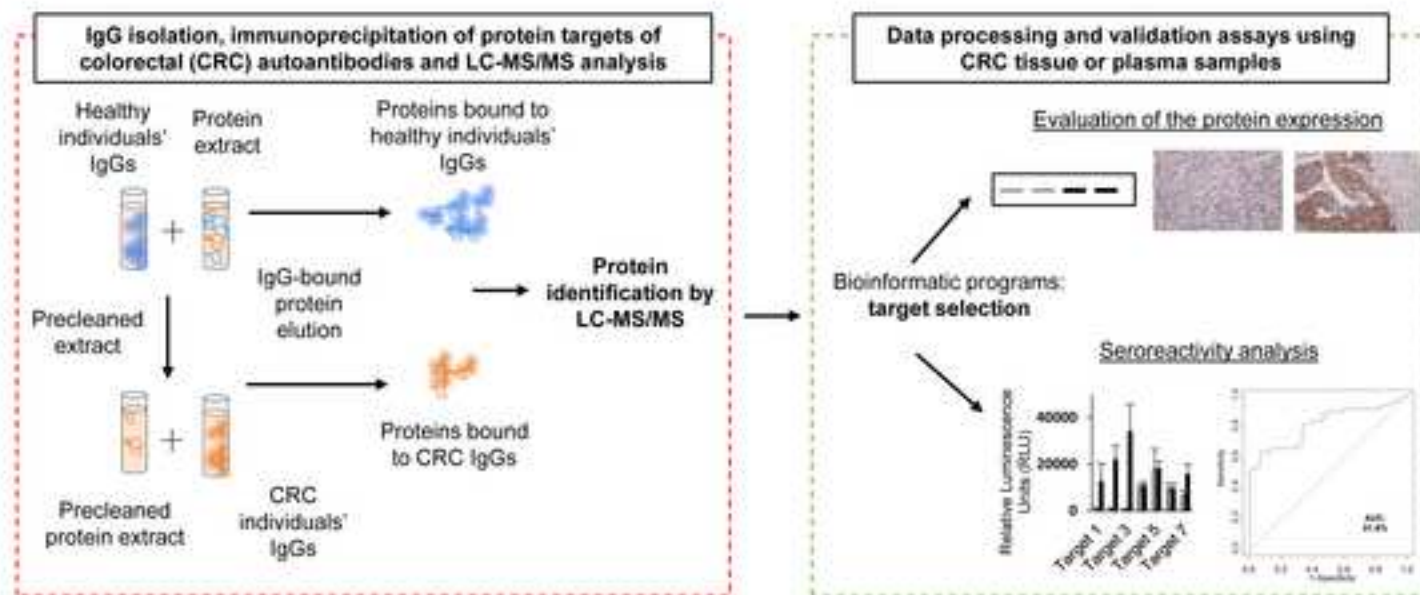
Corresponding Author's Institution: Instituto de Salud Carlos III

First Author: María Garranzo-Asensio

Order of Authors: María Garranzo-Asensio; Pablo San Segundo-Acosta; Carmen Poves; Maria Jesus Fernández-Aceñero; Javier Martínez-Useros, PhD; Ana Montero-Calle; Guillermo Solís-Fernández; Maricruz Sanchez-Martinez; Nuria Rodriguez; María Ángeles Cerón; Servando Fernandez-Diez; Gemma Domínguez; Vivian de los Ríos; Alberto Pelaez-Garcia; Ana Guzmán-Aránguez; Rodrigo Barderas, Chemistry

Abstract: Colorectal cancer (CRC) is the third most common cancer and the second leading cause of cancer related death worldwide. Its diagnosis at early stages would significantly improve the survival of CRC patients. The humoral immune response has been demonstrated useful for cancer diagnosis, predating clinical symptoms up to 3 years. Here, we employed an in-depth seroproteomic approach to identify proteins that elicit a humoral immune response in CRC patients. The seroproteomic approach relied on the immunoprecipitation with patient-derived autoantibodies of proteins from CRC cell lines with different metastatic properties followed by LC-MS/MS. After bioinformatics, we focused on 31 targets of CRC autoantibodies. After WB and IHC validation, ERP44 and TALDO1 showed potential to discriminate disease-free and metastatic CRC patients, and time to recurrence of CRC patients in stage II. Using plasma samples of 30 healthy individuals, 28 premalignant individuals, and 32 CRC patients, nine out of 13 selected targets for seroreactive analysis showed significant diagnostic ability to discriminate either CRC patients or premalignant subjects from controls. Our results suggest that the here defined panel of CRC autoantibodies and their target proteins should be included in CRC blood-based biomarker panels to get a clinically useful blood-based diagnostic signature for CRC detection.

Significance: Colorectal cancer is one of the deadliest cancer types mainly due to its late diagnosis. Its early diagnosis, therefore, is of great importance since it would significantly improve the survival of CRC patients. In our work, the in-depth seroproteomic analysis of colorectal cancer using isolated IgGs from colorectal cancer patients and controls and protein extract of colorectal cancer cells provide the identification of valuable biomarkers with diagnostic and prognostic ability of the disease



- Colorectal cancer (CRC) associated death is mainly related to its late diagnosis
- The humoral immune response predates clinical symptoms up to 3 years
- Immunomic and seroproteomic analyses identified valuable autoantibody CRC biomarkers
- Identified targets of autoantibodies discriminated CRC and premalignant individuals from controls

1 Identification of tumor-associated antigens with diagnostic ability of 2 colorectal cancer by in-depth immunomic and seroproteomic analysis

3
4 María Garranzo-Asensio^a, Pablo San Segundo-Acosta^{a,b}, Carmen Povés^c, María Jesús
5 Fernández-Aceñero^d, **Javier Martínez-Useros^c**, Ana Montero-Calle^a, Guillermo Solís-
6 Fernández^a, Maricruz Sanchez-Martinez^a, Nuria Rodríguez^f, María Ángeles Cerón^d,
7 Servando Fernandez-Diez^c, Gemma Domínguez^g, Vivian de los Ríos^h, Alberto Peláez-
8 Garcíaⁱ, Ana Guzmán-Aránguez^b, Rodrigo Barderas^{a,*}

9
10 ^aChronic Disease Programme, UFIEC, Instituto de Salud Carlos III, Majadahonda E-28220,
11 Madrid, Spain

12 ^bDepartamento de Bioquímica y Biología Molecular, Facultad de Ciencias Químicas,
13 Universidad Complutense de Madrid, E-28040 Madrid, Spain

14 ^cGastroenterology Unit, Hospital Universitario Clínico San Carlos, E-28040 Madrid, Spain

15 ^dSurgical Pathology Department, Hospital Universitario Clínico San Carlos, E-28040 Madrid,
16 Spain

17 ^eTranslational Oncology Division, OncoHealth Institute, Fundacion Jimenez Diaz University
18 Hospital, E-28040 Madrid, Spain

19 ^fMedical Oncology Department, Hospital Universitario La Paz, E-28046 Madrid, Spain

20 ^gDepartamento de Medicina, Facultad de Medicina, Instituto de Investigaciones Biomédicas
21 “Alberto Sols”, CSIC-UAM, E-28029 Madrid, Spain

22 ^hCentro de Investigaciones Biológicas, CSIC, E-28040 Madrid, Spain

23 ⁱSurgical Pathology Department, Hospital Universitario La Paz, E-28046 Madrid, Spain

24
25 *To whom correspondence should be addressed:

26 Rodrigo Barderas.

27 Chronic Disease Programme, UFIEC, Functional Proteomics Unit, Instituto de Salud Carlos III,
28 E-28222 Majadahonda, Madrid, Spain; Tel.: 34-91-8223231; E-mail: r.barderasm@isciii.es

30 Running title

31 CRC biomarker identification by seroproteomic analysis

33 Disclosure of Potential Conflicts of Interest

34 The authors declare no potential conflicts of interest

35
36 Abstract word count: 200

37 Significance word count: 73

38 Text word count: **5901**

39 Tables and Figures: 7

40 Supplementary Tables and Figures: 8

41 **Abstract**

42 Colorectal cancer (CRC) is the third most common cancer and the second leading cause of
43 cancer related death worldwide. Its diagnosis at early stages would significantly improve the
44 survival of CRC patients. The humoral immune response has been demonstrated useful for
45 cancer diagnosis, predating clinical symptoms up to 3 years. Here, we employed an in-depth
46 seroproteomic approach to identify proteins that elicit a humoral immune response in CRC
47 patients. The seroproteomic approach relied on the immunoprecipitation with patient-derived
48 autoantibodies of proteins from CRC cell lines with different metastatic properties followed by
49 LC-MS/MS. After bioinformatics, we focused on 31 targets of CRC autoantibodies. After WB
50 and IHC validation, ERP44 and TALDO1 showed potential to discriminate disease-free and
51 metastatic CRC patients, and time to recurrence of CRC patients in stage II. Using plasma
52 samples of 30 healthy individuals, 28 premalignant individuals, and 32 CRC patients, nine out
53 of 13 selected targets for seroreactive analysis showed significant diagnostic ability to
54 discriminate either CRC patients or premalignant subjects from controls. Our results suggest
55 that the here defined panel of CRC autoantibodies and their target proteins should be included in
56 CRC blood-based biomarker panels to get a clinically useful blood-based diagnostic signature
57 for CRC detection.

58 1. Introduction

59 Colorectal cancer is the second cause of cancer death in Europe, mainly due to its late
60 diagnosis. If CRC patients were early diagnosed, the percentage of treatable cured patients
61 would greatly increase to 80-95% of patients. However, only around 37% of CRC patients are
62 diagnosed at an early stage, leading to a drop in patient survival from 80-95% to 50 or even 6-
63 10% for CRC diagnosis at stage III and IV respectively [1]. It is vital thus to improve the
64 current scenario for early CRC detection consequently increasing patient survival. In this sense,
65 evidence from several studies has shown that CRC screening is effective and economical in
66 average-risk population [2]. Therefore, the development of accurate blood-based biomarker
67 panels is mandatory for the early diagnosis of the disease.

68 The humoral immune response has been proven to play an important role in CRC. Indeed,
69 numerous tumor-associated antigens (TAAs) target of autoantibodies produced by the immune
70 system of CRC patients have been identified by protein microarrays-based proteomic techniques
71 [3]. Since autoantibodies can be detected at early cancer stages, they can be exploited to
72 increase the percentage of CRC patients early diagnosed [4]. However, new biomarkers and
73 diagnostic platforms are needed to reach enough sensitivity and specificity to get a clinically
74 useful blood-based diagnostic signature of CRC based on autoantibodies.

75 Up to date, CRC TAAs have been mainly identified through protein microarrays-based
76 proteomic techniques such as natural and recombinant protein microarrays and phage
77 microarrays [5, 6]. Such techniques are mainly hindered by the limited identification of
78 dysregulated proteins to those printed onto the array. Unfortunately, the set of proteins that can
79 be found in commercial microarrays encompasses only between 50% to 66% of all human
80 proteins without their PTMs and proteoforms. Then, whether the missing proteins are potential
81 CRC biomarkers cannot be evaluated.

82 In our aim to extend the number of identified CRC TAAs, we set up an immunomic and
83 seroproteomic approach to find protein targets of CRC patients' autoantibodies (IgGs) using
84 CRC cell lines protein extracts. Immunoprecipitated proteins bound to CRC IgGs were
85 identified by LC-MS/MS using a Q-exactive and screened by bioinformatics to find actual

86 targets of CRC autoantibodies. A total of 13 out of 79 proteins identified as potential targets of
87 CRC IgGs were selected for validation by: i) extensive meta-analysis to determine their
88 potential dysregulation in CRC, ii) WB and IHC to determine if their potential dysregulation
89 could be associated to prognosis of CRC patients, and iii) seroreactive analysis to determine
90 their diagnostic effectiveness using a collection of 80 individual plasma samples of healthy
91 individuals, premalignant subjects with low- and high-grade colorectal adenomas, and CRC
92 patients. In this sense, it was demonstrated that 9 out of the 13 selected proteins for validation
93 were actual targets of CRC IgGs, with significant diagnostic ability to discriminate either CRC
94 patients at late stages or premalignant subjects from control individuals.

95 2. Material and Methods

96

97 2.1. Colorectal cancer cell culture and lysate production

98

99 SW480 and SW620 cell lines from the American Type Culture Collection cell repository,
100 and KM12C and KM12SM cell lines from I. Fidler's laboratory (MD Anderson Cancer Center),
101 were grown according to established protocols. For protein extract preparation, cells were lysed
102 with RIPA buffer (Sigma) containing protease inhibitors.

103

104 2.2. Immunoprecipitation of protein targets of IgGs from CRC patients

105

106 Sera pools (100 µl) containing three and five sera from CRC stage III and IV, respectively
107 (CRC pool), or eight sera from healthy individuals with negative colonoscopy (healthy pool)
108 were used (Table 1; Supplementary Table S1). For IgG isolation, sera pools were separately
109 incubated in 600 µl 20 mM sodium phosphate pH 7 with 200 µl of protein G agarose beads for
110 90 min at room temperature and gentle rotation. After incubation, protein G agarose beads were
111 washed six times with 600 µl 20 mM sodium phosphate pH 7. Bound IgGs were then eluted
112 with 300 µl 0.1 M glycine pH 2.7, and neutralized with 1 M Tris pH 8.8. Isolated IgGs were
113 visualized by Coomassie Blue staining after SDS-PAGE, and its concentration measured.

114 Next, 200µg of purified IgGs from healthy and CRC pools were separately incubated during
115 2 h with 100 µl of protein G agarose beads in 600 µl of TBS buffer pH 7.4. Then, beads were
116 washed with 200 mM methylamine pH 8.9 prior to the covalent binding of the IgGs to the
117 agarose beads with 50 mM DMP for 1 h at room temperature at 25 rpm. Then, beads were
118 washed with 600 µl of triethanolamine and blocked with 600 µl of ethanolamine, and non-
119 covalently bound IgGs eluted with 400 µl of 0.1 M glycine in 2 M urea pH 2.7, and equilibrated
120 afterwards with 100 µl of TBS buffer pH 7.4. Then, for immunoprecipitation of seroreactive
121 proteins, 5 mg of CRC cells protein extracts were pre-cleaned using 20 µl of Protein G agarose
122 beads previously equilibrated in RIPA buffer, and then incubated overnight with the healthy

123 IgGs covalently bound to beads. Next, the pre-cleaned protein extract was collected and the
124 beads with IgGs from healthy individuals were washed ten times with 600 µl of washing buffer
125 (TBS-0.2% triton). Beads were then centrifuged, and bound proteins eluted with 100 µl 0.1 M
126 glycine pH 2.7 and subsequently neutralized with 20 µl of 2 M ammonium bicarbonate pH 8.8.

127 Finally, for the identification of proteins seroreactive to CRC patients IgGs, the pre-cleaned
128 extract was incubated with the agarose beads covalently bound with the CRC patients IgGs, and
129 proteins were eluted **as above described**. For protein identification by LC-MS/MS, 50% of the
130 eluted content was concentrated onto a SDS-PAGE and in-gel digested with trypsin according
131 to established protocols [7-11].

132

133 2.3. LC-MS/MS analysis

134

135 All peptide separations were carried out on an Easy-nLC 1000 nano system (Thermo
136 Scientific). For each analysis, samples were loaded into a precolumn Acclaim PepMap 100
137 (Thermo Scientific) and eluted in a RSLC PepMap C18, 15 cm long, 50 µm inner diameter and
138 2 µm particle size (Thermo Scientific). The mobile phase flow rate was 300 nL/min using 0.1%
139 formic acid in water (solvent A) and 0.1% **formic acid in acetonitrile** (solvent B). The gradient
140 profile was set as follows: 0%-35% solvent B for 90 min, 35%-100% solvent B for 4 min, 100%
141 solvent B for 8 min. Four microliters of each sample **were** injected.

142 MS analysis was performed using a Q Exactive mass spectrometer (Thermo Scientific). For
143 ionization, 2000 V of liquid junction voltage and 270 °C capillary temperature **were** used. The
144 full scan method employed a m/z 400-1500 mass selection, an Orbitrap resolution of 70,000 (at
145 m/z 200), a target automatic gain control (AGC) value of 3e6, and maximum injection times of
146 100 ms. After the survey scan, the 15 most intense precursor ions were selected for MS/MS
147 fragmentation. Fragmentation was performed with a normalized collision energy of 27 and
148 MS/MS scans were acquired with a starting mass of m/z 100, AGC target was 2e5, resolution of
149 17,500 (at m/z 200), intensity threshold of 8e3, isolation window of 2 m/z units and maximum
150 IT was 100 ms. Charge state screening was enabled to reject unassigned, singly charged, and

151 greater than or equal to seven protonated ions. A dynamic exclusion time of 20s was used to
152 discriminate against previously selected ions.

153

154 *2.4. MS data analysis*

155

156 MS data were analyzed with Proteome Discoverer (version 1.4.1.14) (Thermo Scientific)
157 using standardized workflows. Mass spectra *.raw files were searched against
158 SwissProt_2016_10.fasta, Homo sapiens (human) database (20121 sequences protein entries)
159 using Mascot (version 2.6.0, Matrix Science) search engine. Precursor and fragment mass
160 tolerance were set to 10 ppm and 0.02 Da, respectively, allowing 2 missed cleavages,
161 carbamidomethylation of cysteines as fixed modification, and methionine oxidation, Acetyl (N-
162 term) and Phosphorylation (S, T, Y) as variable modifications. Identified peptides were filtered
163 using Percolator algorithm with a q-value threshold of 0.01 [12].

164

165 *2.5. Bioinformatics analysis*

166

167 Identified proteins appearing in more than 10% of agarose-based immunoprecipitation
168 experiments reported in CRAPome (Contaminant Repository for Affinity Purification Mass
169 Spectrometry Data) data base were considered false positives [13]. Bioinformatics analysis of
170 proteins passing this criterion was performed using STRING and IPA Analysis (Ingenuity
171 Systems) to identify altered networks and pathways [14]. STRING Version 9.1 and MCL
172 clustering enrichment 2 with the default 0.4 confidence score were used to identify the
173 interacting partners in the dataset.

174 To examine whether protein or genetic alterations associated to CRC had been previously
175 associated with identified proteins out of CRAPome, we performed extensive meta-analysis
176 using the Oncomine [15], UALCAN [16], and cBioPortal [17] databases, which give
177 information on differential protein expression, heatmaps of selected dysregulated genes, and
178 identified genetic alterations in tumor tissue samples, respectively. To evaluate whether the

179 identified proteins had been previously associated with disease prognosis, information was
180 retrieved from the Human Protein Atlas [18, 19].

181

182 2.6. Gateway plasmid construction, gene cloning, DNA preparation and protein expression

183

184 Sequence-verified, full-length cDNA plasmid containing selected targets for validation
185 (Supplementary Table S2) in flexible pDONR221 or pENTR223 vectors was obtained from the
186 publicly available DNASU Plasmid Repository [20]. The ORFs were transferred by LR clonase
187 reactions (Invitrogen, Carlsbad, CA) to the pANT7_cHalo expression vector for *in vitro* protein
188 expression to get the autoantigens expressed as fusion proteins to HaloTag in the C-terminal
189 [21-23]. As controls, we also obtained the expression vectors for producing HaloTag protein.
190 All donor and expression plasmids were sequence verified prior to a subsequent use.

191 Proteins were expressed using the 1-Step Human Coupled IVT Kit HeLa cell lysate (Thermo
192 Fisher Scientific, Waltham, MA) as per manufacturer's recommendations.

193

194 2.7. RNA Extraction and semi-quantitative PCR

195

196 RNA was extracted from 5×10^7 cells with the RNeasy Mini Kit (Qiagen) and quantified with
197 a NanoDrop ND-1000 spectrophotometer (Thermo Fisher Scientific). cDNA was synthesized
198 using the NZY First-Strand cDNA Synthesis Kit, separate oligos (NZYTech). For semi-
199 quantitative reverse transcriptase-PCR (RT-PCR), reactions were performed using specific
200 primers (Supplementary Table S3) and the Phusion High-Fidelity DNA Polymerase (Thermo
201 Fisher Scientific), according to the manufacturer recommendations. PCR products were
202 separated on 1.5% agarose gel containing GelRed (Biotium). GAPDH was used as internal
203 control.

204 2.8. *SDS-PAGE and WB analysis*

205

206 SDS-PAGE and WB analyses were performed as previously reported [24]. Alternatively,
207 0.67 µl of the *in vitro* protein extracts or 10µg of protein extracts were run in 10% SDS-PAGE
208 and transferred to nitrocellulose membranes (Hybond-C extra). After blocking, membranes were
209 incubated with optimized dilutions of indicated specific monoclonal or polyclonal antibodies
210 (Supplementary Table S4). Immunodetection on membranes was achieved by using HRP-
211 conjugated secondary antibodies (Supplementary Table S4). Chemiluminescence signal was
212 developed with ECL Western Blotting Substrate (Thermo Scientific) and detected on an
213 Amersham Imager 680 (GE Healthcare).

214

215 2.9. *Patient plasma*

216

217 The Institutional Ethical Review Boards of the Instituto de Salud Carlos III, Hospital Clínico
218 San Carlos (Madrid), and La Paz Hospital (Madrid) approved this study on biomarker discovery
219 and validation (CEI PI 45). Plasma samples were obtained from the biobanks of the Hospital
220 Clínico San Carlos (IdISSC) and La Paz Hospital (IdIPAZ), which belongs to the National
221 Biobank Net (ISCIII) cofounded with FEDER funds, after approval of the Ethical Review
222 Boards of these institutions. Written informed consent was obtained from all patients. Plasma
223 samples were collected using a standardized sample collection protocol and stored at -80°C until
224 use [4, 25-27].

225 For seroreactive analysis, 32 plasma samples from CRC patients, 18 from premalignant
226 subjects (low- or high-grade adenomas in the colon), and 30 from control individuals
227 (individuals asymptomatic and negative colonoscopy individuals, or individuals with fecal
228 occult blood test -FOBT- positive and negative colonoscopy) were used (Table 1;
229 Supplementary Table S1).

230 2.10. Seroreactive analysis

231

232 HaloTag fusion proteins coupled to **Magne HaloTag beads (MBs, Promega)** and ELISA-like
233 immunoassay was previously optimized to measure autoantibodies [11, 22]. Briefly, for each
234 reaction, a relation of 0.67 μL of the *in vitro* protein expression was incubated with 0.5 μL of
235 **MBs** suspension overnight at 4°C for protein capture to MBs according to manufacturer
236 instructions. For covalent binding, a mixture of the required amount of protein and **MBs** was
237 made taking into account the number of replicates and measurements to be performed. After
238 three washing steps with PBS, Triton X-100 0.05%, Tween 20 0.1% **rocking for 5 min at 250**
239 **rpm**, unbound proteins were removed adding 100 μL of glycine 0.1 M pH 2.7 for 5 min at RT
240 and 250 rpm shaking. Then, HaloTag fusion proteins immobilized in MBs were blocked with
241 SuperBlock for 1h and then transferred onto separate wells of Bio-Plex 96-well plates to
242 perform subsequent incubations overnight with pooled or individual plasma samples at
243 indicated dilutions in PBS supplemented with Tween 20 0.1% (v/v) **and BSA 3%** (w/v). After
244 extensive washing as above, HRP-conjugated anti-human IgG antibody (Jackson) diluted
245 1:10000 in PBS supplemented with Tween 20 0.1% (v/v) **and BSA 3%** (w/v) was incubated to
246 detect the presence of autoantibodies. Alternatively, to verify the TAA-HaloTag
247 immobilization, HaloTag was detected with the monoclonal anti-HaloTag antibody (Promega)
248 **diluted 1:1000**, followed by 1h of incubation with HRP- conjugated anti-mouse IgG diluted
249 1:2500. To develop the chemiluminescence signal, MBs were incubated on black Maxisorp 96-
250 well plates (Nunc) with 50 μL of SuperSignal ELISA Pico Maximum Sensitivity Substrate
251 (Pierce) for 1 min. Then, signal was recorded on The Spark multimode microplate reader (Tecan
252 Trading AG).

253

254 2.11. Tissue Microarrays and immunohistochemistry

255

256 Core tumor tissue samples from 50 metastatic and non-metastatic CRC patients and core
257 tumor tissue samples from 94 recurrent or non-recurrent CRC stage II patients composed the

258 two TMAs used in the study. Immunohistochemical staining using optimized antibody dilutions
259 (Supplementary Table S4), visualization and immunoreactivity was conducted according to
260 established protocols [4, 14, 25, 27].

261

262 2.12. *Statistical analysis*

263

264 Statistical analyses were performed with Microsoft Office Excel. For the seroreactive and
265 immunohistochemistry analysis, data distribution using the Shapiro-Wilk test and variance
266 homogeneity using the Bartlett test was first evaluated. Since data normality was discarded in
267 all cases, we then assessed whether the means of control individuals, and premalignant
268 individuals and/or CRC patients were statistically different from each other using the non-
269 parametric U-Mann Whitney test assuming unequal variances. p-values <0.05 were considered
270 statistically significant. The diagnostic capacity of each individual protein as well as their
271 combination was evaluated by a receiver operating characteristic (ROC) curve. ROC curves and
272 the corresponding area under the curve (AUC) and the maximized sensitivity and specificity
273 values were obtained with the R program (version 3.2.3) using the R package Epi [28].

274 3. Results

275

276 In the present study, we aimed at developing a methodological approach to identify tumor-
277 associated antigens through immunoprecipitation of potential autoantibody targets using IgGs
278 from CRC patients at stages III and IV and healthy individuals. The isolated IgGs were
279 separately incubated with protein extracts from CRC isogenic cell lines with different metastatic
280 properties and, then, immunoprecipitated and subsequently identified by mass spectrometry.
281 SW480 and KM12C CRC cells were used as model of primary tumor and SW620 and
282 KM12SM cells as model of metastatic CRC to lymph nodes and liver, respectively. A schematic
283 representation of the workflow of the study is depicted (Fig. 1).

284

285 *3.1. Identification of seroreactive proteins to IgGs from CRC patients by immunoprecipitation*
286 *followed by LC-MS/MS*

287

288 For IgG isolation, plasma samples from healthy individuals with negative colonoscopy and
289 unknown pathology (control group), and plasma samples from CRC patients at stages III and IV
290 obtained before surgery (CRC group) were separately pooled (Table 1).

291 The analyzed protein extract (10 mg) was obtained by mixing equal amounts of cell lysates
292 from KM12C, KM12SM, SW480, and SW620 cells. The IgGs obtained from healthy
293 individuals were used to pre-clean the protein extract, which was then incubated with IgGs from
294 CRC patients to identify specific CRC seroreactive proteins.

295 Both protein fractions seroreactive to IgGs from healthy and/or CRC patients were firstly
296 analyzed by SDS-PAGE followed by silver staining, and then, by mass spectrometry for the
297 identification of CRC TAAs.

298 First, by SDS-PAGE and silver-staining, a differential staining at high- and low-molecular
299 weight was observed when comparing protein bands from the eluted seroreactive proteins to
300 IgGs from healthy and CRC patients (Fig. 1). Then, the eluted proteins from both IgGs were
301 concentrated in parallel by SDS-PAGE and in-gel digested with trypsin for subsequent mass

302 spectrometry analysis (Fig. 1). In total, 442 proteins were identified in both experiments. From
303 the set of identified proteins, 203 were found to be common to both control and CRC
304 conditions, while 160 and 79 were identified only in the control or in the CRC
305 immunoprecipitation, respectively (Supplementary Table S5).

306

307 3.2. Bioinformatics of the seroreactive proteins to CRC IgGs

308

309 Next, the set of CRC specific proteins was subjected to an extensive meta-analysis with
310 different bioinformatic tools to identify those that were more likely to be actual CRC
311 autoantibody targets, and thus potential disease biomarkers.

312 First, CRAPome was used to remove false positive seroreactive proteins target of
313 autoantibodies. Using a cut-off of <10% of appearance in recorded mass spectrometry analysis
314 of immunoprecipitation experiments using agarose beads, 31 proteins were found more prone to
315 be actual CRC autoantibody targets (Table 2). Remarkably, the well-documented cancer
316 autoantibody p53 appeared among the 31 proteins [29], suggesting that our approach would be
317 useful for the identification of CRC-specific TAAs.

318 It has been reported that proteins target of autoantibodies are usually overexpressed and/or
319 mutated. Therefore, we used the cBioPortal, Oncomine and UALCAN databases to investigate
320 whether alterations related to these proteins at a genetic and/or protein level had been previously
321 associated to CRC. We searched for recorded genetic alterations in the TCGA CRC database in
322 cBioPortal. Interestingly, 69% and 80% of the identified targets had genetic alterations
323 (mutation, amplification, deep deletion, and other alteration) in colon and rectal
324 adenocarcinomas, respectively (Fig. 2A). We then used the Oncomine and UALCAN databases
325 to find any dysregulation in the expression of the proteins at tissue level in CRC. We found that
326 22 out of the 31 identified proteins showed a statistically significant altered expression ($p < 0.05$)
327 in CRC in comparison to adjacent paired healthy tissue (Fig. 2B), with 17 of them showing
328 upregulation in colorectal tumoral tissue (Fig. 2B). Moreover, one of the identified proteins,

329 CTTNBP2NL, was found to be a CRC prognosis marker in the Pathology Atlas from the
330 Human Protein Atlas (Fig. 2C).

331 Finally, String database and IPA were used to identify possible altered cell functions and
332 molecular pathways. With String, proteins were clustered by direct and indirect interactions,
333 obtaining 5 interacting groups composed of proteins related to i) GTPases and actin-interacting
334 proteins; ii) transcription, immunity and cell cycle functions; iii) pentose pathway and
335 endoplasmic reticulum; iv) respiratory chain and caspase activity; and v) respiratory chain and
336 cell messengers (Supplementary Fig. 1A). These functions, related to immune response, actin
337 interaction and cell death, have been closely associated to cancer. Among the networks found to
338 be altered with IPA, some were related to highly altered processes in cancer such as cell cycle,
339 DNA replication, recombination, protein synthesis and carbohydrate metabolism
340 (Supplementary Fig. 1B).

341 Collectively, these data show that the identified proteins that are potential targets of CRC
342 autoantibodies are dysregulated at a genetic and/or protein level in CRC. Furthermore, their
343 dysregulation plays an important role in the alteration of molecular pathways and cellular
344 functions related to the pathology.

345

346 3.3. Genetic and protein expression verification in CRC cell lines

347

348 From the 31 remaining proteins after CRAPome screening, 13 were selected for validation at
349 mRNA and protein level (Table 2). The criteria for this selection were antibody and cDNA
350 availability together with existing information (i.e. whether they had already been described as
351 TAAs in other cancer types). Plasma or secreted proteins were discarded for further validation.

352 We verified the presence of the targets either at mRNA or protein level in the cell lines used
353 in the study. The presence of all 13 selected targets for validation was confirmed at mRNA level
354 (Supplementary Fig. 2A). ERP44, SCGD1B2, TALDO1, and TRIM29 were also found at the
355 protein level (Supplementary Fig. 2B).

356

357 3.4. Evaluation of protein expression dysregulation in CRC tissue samples as biomarker
358 prognostic assessment

359

360 Next, since TAAs are usually highly dysregulated at protein level in CRC tissue, we
361 evaluated if those proteins validated at protein level in CRC cells might show any dysregulation
362 in tissue and whether they show any diagnostic or prognostic ability. To this end, ERP44,
363 SCGD1B2, TALDO1, and TRIM29 protein abundance was evaluated by IHC using two
364 different TMAs related to metastasis or recurrence of CRC. All proteins showed staining in
365 CRC tissue in both TMAs, indicating a clear presence of the proteins in the pathological tissue
366 samples. TALDO1 showed nuclear staining, while ERP44, SCGD1B2 and TRIM29 showed
367 cytoplasmic staining (Fig. 3A). Moreover, both epithelial and stromal staining was observed for
368 TALDO1, ERP44, and SCGDIB2, while TRIM29 showed only epithelial staining.

369 Interestingly, ERP44 could statistically discriminate between CRC liver metastatic patients
370 according to their survival status ($p=0.049$) (Fig. 3B). In addition, both TALDO1 and ERP44
371 could significantly discriminate between stage II CRC patients according to their recurrence
372 status ($p=0.024$) or according to the time to recurrence ($p=0.039$), respectively (Fig. 3B). Next,
373 to evaluate whether these targets could be useful markers of the disease at protein level, ROC
374 curves were calculated. For the metastatic TMA, when grouping patients according to survival
375 status ERP44 showed an AUC of 70% (40% sensitivity, 100% specificity). For the stage II CRC
376 TMA, when grouping patients according to recurrence status TALDO1 showed an AUC of
377 63.4% (56.9% sensitivity, 66.7% specificity). Finally, when grouping patients according to time
378 to recurrence, the AUC of ERP44 was 61.4% (59.1% sensitivity, and 65.9% specificity) (Fig.
379 3C).

380 Collectively, these results highlight that the dysregulation of proteins seroreactive to IgGs
381 from CRC patients show potential to discriminate metastatic CRC patients, recurrence and time
382 to recurrence of CRC patients in stage II.

383 3.5. Cloning, *in vitro* protein expression and seroreactive analysis of the potential CRC TAAs

384

385 Our research hypothesis relied on the identification of proteins target of autoantibodies in
386 CRC with diagnostic ability. To address this question, we evaluated the presence of cancer
387 autoantibodies in plasma samples from CRC patients, premalignant subjects, and control
388 individuals, and determine their diagnostic ability.

389 To this end, the 13 selected targets were cloned in the pANT7_cHalo expression vector for
390 their *in vitro* expression as HaloTag fusion proteins [22]. Then, we confirmed the *in vitro*
391 expression of the TAAs as fusion proteins to HaloTag, and the correct covalent immobilization
392 of the fusion proteins in MBs (Fig. 4A). All proteins were visualized by immunostaining after
393 SDS-PAGE at the theoretical molecular mass of the fusion protein. In addition, all of them were
394 able to covalently bind to chloroalkane functionalized MBs (data not shown), and thus, they
395 should be able to be recognized by CRC autoantibodies in an ELISA-like test [11, 22, 30].

396 Next, we analyzed the seroreactivity to these 13 potential TAAs using 80 individual plasma
397 samples (30 from control individuals, 28 from premalignant subjects, and 32 from stage III and
398 IV CRC patients). We found that CRC patients possess significantly higher levels of
399 autoantibodies than control individuals, whose levels were always lower or undetectable (Fig.
400 4B). However, only autoantibodies against CHCHD3, CTTNBP2NL, FKBP4, MGST3,
401 THSD7A, TRIM29 -as well as p53- showed a statistically significant difference (p-values
402 <0.01) comparing the asymptomatic healthy control group and the CRC group (Fig. 4C). In
403 addition CTTNBP2NL, FKBP4, and TALDO1 autoantibody levels were able to significantly
404 discriminate between asymptomatic healthy controls and premalignant subjects (p-value < 0.01)
405 (Fig. 4D). Finally, ERP44, TALDO1, CHCHD3, CTTNBP2NL, FKBP4, MGST3, THSD7A,
406 and TRIM29 -as well as p53- were able to discriminate between the asymptomatic healthy
407 individuals and the colorectal pathological group (p-value<0.04 (Fig. 4E).

408 3.6. Evaluation of the diagnostic value of CRC autoantibodies

409

410 Finally, the diagnostic value of the CRC TAAs was evaluated by means of ROC curves.
411 AUC, sensitivity and specificity values were calculated individually or in combination using
412 those autoantibodies showing significant levels in above comparisons.

413 CHCHD3, CTTNBP2NL, FKBP4, MGST3, THSD7A, and TRIM29 showed an individual
414 AUC higher than 70% to discriminate between CRC patients and control individuals
415 (Supplementary Table S6). In combination, the AUC increased to 99.7%, with a sensitivity of
416 96.9% and specificity of 100% (Fig. 5A). In addition, autoantibodies against CTTNBP2NL,
417 FKBP4, and TALDO1 could discriminate between control individuals and premalignant
418 subjects with an individual AUC higher than 71.9% (Supplementary Table S6), and in
419 combination the AUC increased to 88.9% with a sensitivity of 83.3% and specificity of 86.7%
420 (Fig. 5B). Finally, CHCHD3, CTTNBP2NL, ERP44, FKBP4, MGST3, TALDO1, THSD7A,
421 and TRIM29 showed an individual AUC higher than 59.2% to discriminate between control
422 individuals and the pathological group, and their combination with p53 led to a combined AUC
423 of 95.3%, with a sensitivity of 92.0% and a specificity of 90.0% (Fig. 5C).

424 Collectively, these results highlight the usefulness of the followed approach to identify
425 TAAs with significant diagnostic ability. In addition, our results suggest that the here defined
426 CRC TAAs should be included in a CRC blood-based biomarker panel to get a clinically useful
427 blood-based diagnostic signature for CRC detection.

428 4. Discussion

429

430 Protein microarrays are a highly renowned used technique for identifying protein-protein
431 interactions, drug and small-molecule screening, epitope mapping, host-pathogen interactions
432 ... [31-34]. However, protein microarrays have been mainly used for the identification of
433 tumor-associated antigens in cancer malignancies [31-35]. Although theoretically the whole
434 proteome might be printed in protein microarrays, the highest density achieved so far is about
435 75% of the human proteome -considering one ORF per protein but without multiple
436 proteoforms of the same protein- [36-38]. Alternatively, high-density PrESTs arrays covering
437 approximately the whole proteome has been produced [38]. However, in this case medium to
438 large peptides of about 90% of all human ORF proteins are printed in the arrays, with the
439 limitation that in these arrays 3D non-linear relevant epitopes, and thus relevant TAAs, might be
440 lost during the screening.

441 Therefore, although protein microarrays have been demonstrated highly useful in identifying
442 CRC autoantibodies and their target proteins, new methodologies need to be applied to achieve
443 the completion in the identification of TAAs. Here, we investigated whether a modified SASI
444 methodology without SILAC labeling of cells based on mass spectrometry [39], which have
445 been useful for identifying targets of IgGs in vaccinated pancreatic cancer patients with a
446 granulocyte-macrophage colony stimulating factor (GM-CSF) secreting pancreatic cancer
447 vaccine (GVAX) in phase II clinical trials [39], might help in elucidating new CRC TAAs using
448 IgGs isolated from the plasma of CRC patients and protein extracts from CRC cell lines.

449 Previous studies applying mass spectrometry approaches have permitted the identification of
450 autoantibodies against TAAs in different types of cancer, including CRC [40-42]. However,
451 these studies have been mainly focused on combining immunoblotting of protein extracts
452 separated by 2DE-gels using patients' sera for identification of reactive spots and their
453 subsequent protein identification by mass spectrometry, limiting the identification to medium or
454 highly abundant TAAs. Here, the SASI modified approach combining immunoprecipitation
455 directly coupled to LC-MS/MS allowed for the identification of autoantibodies and their target

456 proteins in colorectal cancer. The use of immunoprecipitation to capture the reactive TAAs in
457 solution having the proteins their *a priori* 3D conformation **instead of blotting them after their**
458 **separation by 2DE-gel** confers some advantages. Mainly, there is no limitation on protein
459 isolation by immunoprecipitation for further identification *via* LC-MS/MS. All reactive proteins
460 to the immobilized antibodies are bound independently on their concentration, while 2DE-MS is
461 not useful to identify low abundant proteins. Moreover, reactive spots proceeding from 2DE
462 have conformational limitations since they are bound onto membranes and discontinuous
463 reactive epitopes are lost. Since previous studies have revealed that the immune response
464 against proteins, apart from being patient specific, is highly polyclonal and mainly produced
465 against 3D discontinuous epitopes [23, 35]. This last limitation could produce the
466 misidentification of relevant TAAs, which could be overcome by immunoprecipitation. Here,
467 among the identified proteins as potential autoantibody targets in CRC (Table 2), we observed
468 the presence of at least one protein **containing continuous** and discontinuous epitopes -p53-, as it
469 has been previously demonstrated by ELISA, WB and protein microarrays [23, 29, 43], and thus
470 supporting our approach to identify TAAs avoiding conformational limitations.

471 Here, we have validated our protein dataset by meta-analysis of databases related to CRC.
472 Twenty-two out of 31 identified proteins were observed to present a genetic alteration or altered
473 expression at mRNA or protein level in the disease. In addition, by IHC TALDO1, and ERP44
474 protein abundance in CRC tissue could discriminate between metastatic and **non-metastatic**
475 patients and between recurrent and **non-recurrent** patients, or according to the time to
476 recurrence. These alterations have been defined as the ones producing a humoral immune
477 response in cancer patients to overproduce autoantibodies against them [35].

478 Of our identified validated dataset, several markers have been found to play a potential role
479 in cancer. CHCHD3, a component of the mitochondrial inner membrane complex MICOS,
480 plays an important role in the maintenance of its stability and in mitochondrial morphological
481 stability [44]. To our knowledge, there is only one study that has linked its dysregulation with
482 **early cancer diagnosis [45], but in pancreatic cancer**. Regarding CTTNBP2NL, it has been
483 shown dysregulated in a genetic study of oral squamous cell carcinoma [46]. ERP44, a protein

484 that reportedly regulates calcium release into the endoplasmic reticulum, has shown that it
485 modulates lung cancer cell migration [47], and that its knock-down inhibited mammosphere
486 growth of breast cancer cells [48]. On the other hand, MGST3, TALDO1, TRIM29, and
487 THSD7A had been previously reported as potential cancer markers in different studies by the
488 evaluation of their expression levels. However, no studies focusing on them as target of
489 autoantibodies and/or their potential use as blood-based biomarkers for cancer diagnosis have
490 been described. Only autoantibodies against THSD7A have been previously described to
491 classify membranous nephropathy and **to be associated to** outcome and treatment response [49].
492 MGST3, a protein with antioxidant functions by reducing GSH, has been reported as biomarker
493 for oral squamous cancer [50]. **It is highly up-regulated** in basal-like breast cancer cell lines, **and**
494 **thus, makes** it a possible triple-negative breast cancer biomarker [51]. TALDO1, **an important**
495 **protein for the balance of metabolites in the pentose pathway**, has been previously identified by
496 proteomic techniques to be a potential biomarker in non-small cell lung cancer [52]. **In addition,**
497 **it has** also been identified to be upregulated in pancreatic cancer [53]. However, there is no
498 information on its possible role in CRC. On the other hand, TRIM29, which plays an important
499 role on the regulation of macrophage activation against bacterial and viral infections within the
500 respiratory tract, has been associated to multiple cancer types [54, 55]. Its upregulation has been
501 described to promote cell proliferation, **poor** prognosis, and aggressiveness in CRC [56].
502 THSD7A is involved in vascular invasion, metastasis and angiogenesis and plays a role in actin
503 cytoskeleton rearrangement [57]. Lastly, the immunophilin protein FKBP4 has been the only
504 protein identified in this study previously reported in other studies as CRC serum antigen [58,
505 59].

506 One of the goals of the study consisted of the discovery of TAAs useful for CRC detection,
507 which might be used as an effective and efficient strategy for the blood-based CRC screening
508 for population at risk (>50 years old). We used pooled samples from CRC patients to avoid
509 potential aberrations and biological variations in the humoral immune response of CRC patients
510 appearing in individual samples, which might increase the capacity to identify the most

511 significant and consistent proteins target of autoantibodies between pooled samples from well-
512 characterized CRC patients in comparison to control individuals. Interestingly, although most of
513 the identified CRC TAAs have been described as **dysregulated** in other cancers, **there are no**
514 **studies focusing on them as target of autoantibodies (except for FKBP4) and/or their potential**
515 **as blood-based biomarkers for cancer diagnosis, including colorectal cancer. Therefore, we**
516 **could achieve the specific CRC detection at early cancer stages by a simple blood test, avoiding**
517 **at the same time the detection of other cancer malignancies by integrating them in a multiplexed**
518 **panel including (if needed) other CRC-specific TAAs targets of autoantibodies to increase as**
519 **much as possible the specificity and sensitivity of the test, especially for the detection of**
520 **pre-malignant individuals.**

521 Regarding the comparison of the here described panel for CRC detection with that used in
522 clinics, it is worth to remark that there is no useful blood-based colorectal cancer marker for
523 diagnosis and that the actual clinical marker is only recommended for recurrence (CEA).
524 Moreover, the recommended population screening strategies for CRC are based on stool test
525 (FOBT) followed, if positive, by structural examination by colonoscopy. While structural exams
526 detect both cancer and pre-malignant lesions, stool tests mainly identify cancer because of their
527 limited sensitivity to detect low- or high-grade adenomas. Moreover, the relatively low
528 specificity of the initial examination results by means of FOBT produces a high false-positive
529 rate and leads to a significant number of unnecessary colonoscopies. Here, with the identified
530 TAA panel for CRC detection, AUC values of 99.7% and 88.9% were achieved for the
531 detection of CRC patients and pre-malignant subjects in comparison to healthy control
532 individuals, respectively. Regarding the clinical detection by FOBT followed by colonoscopy,
533 usual clinical AUC values are about 70% for CRC detection and 60% for pre-malignant subjects.
534 In addition, in a recent report performing FOBT and measuring at the same time two miRNAs -
535 not yet clinically established-, AUC values for detecting CRC and pre-malignant subjects
536 increase to 93% and 64% [60], respectively. Remarkably, in both cases, our approach was able
537 to improve these results. Therefore, the here described approach might serve for a more accurate

538 detection of those patients that should undergo colonoscopy or surgery for the resection of
539 colorectal cancer or premalignant lesions.

540 On the other hand, although it has been provided the unbiased discovery of autoantibody
541 biomarkers validated using individual plasma samples from CRC patients and colorectal
542 premalignant subject in comparison to control individuals, their diagnostic ability should be
543 further validated using **large number of samples and independent patient cohorts**, including
544 blinded samples and samples from other cancer types to assure their CRC specificity and
545 establish their utility for the diagnosis of the disease. In this sense, further research is guaranteed
546 to try to improve the results for the early diagnosis of the disease by multiplexing the here
547 described TAAs and by implementing these biomarkers into a panel containing other previously
548 validated CRC autoantigens in multiplexed bio(sensing) platforms (i.e., biosensors [22],
549 Luminex or protein microarrays) to reach enough sensitivity, specificity, and AUC for the
550 blood-based clinical diagnosis of the disease.

551

552 **5. Conclusions**

553

554 In summary, in this work we propose a CRC blood-based diagnostic signature based on the
555 identification of non-previously defined CRC TAAs by immunoprecipitation of proteins from
556 CRC cell lines and **IgGs** isolated from plasma of CRC patients followed by LC-MS/MS
557 analysis. These candidate TAAs should be part of a multiplex biomarker panel for the blood-
558 based diagnosis of the disease to be further analyzed with samples obtained from longitudinal
559 studies in subjects at the preclinical or early clinical stages of the disease to assure **its** usefulness
560 for early CRC detection.

561

562 Supplementary data to this article can be found online.

563 **Acknowledgments**

564

565 This work was supported by the Ramon y Cajal programme of the MINECO and the
566 financial support of the PI17CIII/00045 grant from the AES-ISCI program to R.B.. M.G-A.
567 was supported by a contract of the Programa Operativo de Empleo Juvenil y la Iniciativa de
568 Empleo Juvenil (YEI) with the participation of the Consejería de Educación, Juventud y
569 Deporte de la Comunidad de Madrid y del Fondo Social Europeo. The FPU predoctoral
570 contracts to P.S.S.-A. and A.M-C. are supported by the Spanish Ministerio de Educación,
571 Cultura y Deporte. G.S-F. is recipient of a predoctoral contract (grant number 1193818N)
572 supported by The Flanders Research Foundation (FWO).

573

574 **Authors' Contributions**

575

576 Conception and design: R.B. Development of methodology: M.G-A., P. SS-A., A.G-A., G.S-
577 F., R.B. Perform Research: C.P., MJ.F-A., J. M-U., A. M-C., G. S-F., N.R., MA.C., G. S-F.,
578 V.R., A.P-G. Analysis and interpretation of data: M.G-A., A.G-A., C.P., MJ.F-A., J. M-U.,
579 V.R., A.P-G., R.B. Writing, review, and/or revision of the manuscript: M.G-A., A.G-A., R.B.
580 Technical, obtaining and processing of samples, or material support: C.P., MJ.F-A., A. M-C.,
581 MA.C., N.R., A.M-C., A.G-A., R.B.

582

583 **Conflicts of interest**

584

585 The authors declare that they have no conflicts of interest.

586 **References**

587

588 [1] Holleczeck B, Rossi S, Domenic A, Innos K, Minicozzi P, Francisci S, et al. On-going
589 improvement and persistent differences in the survival for patients with colon and rectum cancer
590 across Europe 1999-2007 - Results from the EUROCARE-5 study. *Eur J Cancer*. 2015;51:2158-
591 68.

592 [2] Steele RJ, Rey JF, Lambert R, International Agency for Research on C. European guidelines
593 for quality assurance in colorectal cancer screening and diagnosis. First Edition--Professional
594 requirements and training. *Endoscopy*. 2012;44 Suppl 3:SE106-15.

595 [3] Casal JI, Barderas R. Identification of cancer autoantigens in serum: toward
596 diagnostic/prognostic testing? *Mol Diagn Ther*. 2010;14:149-54.

597 [4] Barderas R, Villar-Vazquez R, Fernandez-Acenero MJ, Babel I, Pelaez-Garcia A, Torres S,
598 et al. Sporadic colon cancer murine models demonstrate the value of autoantibody detection for
599 preclinical cancer diagnosis. *Sci Rep*. 2013;3:2938.

600 [5] Barderas R, Babel I, Casal JI. Colorectal cancer proteomics, molecular characterization and
601 biomarker discovery. *Proteomics Clin Appl*. 2010;4:159-78.

602 [6] Barderas R, Villar-Vazquez R, Casal JI. Colorectal Cancer Circulating Biomarkers.
603 *Biomarkers in Cancer Springer Series*. 2014;1:1-21.

604 [7] Barderas R, Mendes M, Torres S, Bartolome RA, Lopez-Lucendo M, Villar-Vazquez R, et
605 al. In-depth characterization of the secretome of colorectal cancer metastatic cells identifies key
606 proteins in cell adhesion, migration, and invasion. *Mol Cell Proteomics*. 2013;12:1602-20.

607 [8] Mendes M, Pelaez-Garcia A, Lopez-Lucendo M, Bartolome RA, Calvino E, Barderas R, et
608 al. Mapping the Spatial Proteome of Metastatic Cells in Colorectal Cancer. *Proteomics*.
609 2017;17.

610 [9] Pelaez-Garcia A, Barderas R, Batlle R, Vinas-Castells R, Bartolome RA, Torres S, et al. A
611 proteomic analysis reveals that Snail regulates the expression of the nuclear orphan receptor
612 Nuclear Receptor Subfamily 2 Group F Member 6 (Nr2f6) and interleukin 17 (IL-17) to inhibit
613 adipocyte differentiation. *Mol Cell Proteomics*. 2015;14:303-15.

614 [10] Pelaez-Garcia A, Barderas R, Mendes M, Lopez-Lucendo M, Sanchez JC, Garcia de
615 Herreros A, et al. Data from proteomic characterization of the role of Snail1 in murine
616 mesenchymal stem cells and 3T3-L1 fibroblasts differentiation. *Data Brief*. 2015;4:606-13.

617 [11] San Segundo-Acosta P, Montero-Calle A, Fuentes M, Rabano A, Villalba M, Barderas R.
618 Identification of Alzheimer's Disease Autoantibodies and Their Target Biomarkers by Phage
619 Microarrays. *J Proteome Res*. 2019.

620 [12] Kall L, Canterbury JD, Weston J, Noble WS, MacCoss MJ. Semi-supervised learning for
621 peptide identification from shotgun proteomics datasets. *Nat Methods*. 2007;4:923-5.

622 [13] Mellacheruvu D, Wright Z, Couzens AL, Lambert JP, St-Denis NA, Li T, et al. The
623 CRAPome: a contaminant repository for affinity purification-mass spectrometry data. *Nat*
624 *Methods*. 2013;10:730-6.

625 [14] Garranzo-Asensio M, San Segundo-Acosta P, Martinez-Useros J, Montero-Calle A,
626 Fernandez-Acenero MJ, Haggmark-Manberg A, et al. Identification of prefrontal cortex protein
627 alterations in Alzheimer's disease. *Oncotarget*. 2018;9:10847-67.

628 [15] Rhodes DR, Yu J, Shanker K, Deshpande N, Varambally R, Ghosh D, et al. ONCOMINE:
629 a cancer microarray database and integrated data-mining platform. *Neoplasia*. 2004;6:1-6.

630 [16] Chandrashekar DS, Bashel B, Balasubramanya SAH, Creighton CJ, Ponce-Rodriguez I,
631 Chakravarthi B, et al. UALCAN: A Portal for Facilitating Tumor Subgroup Gene Expression
632 and Survival Analyses. *Neoplasia*. 2017;19:649-58.

633 [17] Cerami E, Gao J, Dogrusoz U, Gross BE, Sumer SO, Aksoy BA, et al. The cBio cancer
634 genomics portal: an open platform for exploring multidimensional cancer genomics data.
635 *Cancer Discov*. 2012;2:401-4.

636 [18] Uhlen M, Oksvold P, Fagerberg L, Lundberg E, Jonasson K, Forsberg M, et al. Towards a
637 knowledge-based Human Protein Atlas. *Nat Biotechnol*. 2010;28:1248-50.

638 [19] Uhlen M, Fagerberg L, Hallstrom BM, Lindskog C, Oksvold P, Mardinoglu A, et al.
639 *Proteomics*. Tissue-based map of the human proteome. *Science*. 2015;347:1260419.

640 [20] Seiler CY, Park JG, Sharma A, Hunter P, Surapaneni P, Sedillo C, et al. DNASU plasmid
641 and PSI: Biology-Materials repositories: resources to accelerate biological research. *Nucleic*
642 *Acids Res.* 2014;42:D1253-60.

643 [21] Ramachandran N, Raphael JV, Hainsworth E, Demirkan G, Fuentes MG, Rolfs A, et al.
644 Next-generation high-density self-assembling functional protein arrays. *Nat Methods.*
645 2008;5:535-8.

646 [22] Garranzo-Asensio M, Guzman-Aranguez A, Poves C, Fernandez-Acenero MJ, Torrente-
647 Rodriguez RM, Ruiz-Valdepenas Montiel V, et al. Toward Liquid Biopsy: Determination of the
648 Humoral Immune Response in Cancer Patients Using HaloTag Fusion Protein-Modified
649 Electrochemical Bioplatfroms. *Anal Chem.* 2016;88:12339-45.

650 [23] Katchman BA, Barderas R, Alam R, Chowell D, Field MS, Esserman LJ, et al. Proteomic
651 mapping of p53 immunogenicity in pancreatic, ovarian, and breast cancers. *Proteomics Clin*
652 *Appl.* 2016;10:720-31.

653 [24] Barderas R, Shochat S, Timmerman P, Hollestelle MJ, Martinez-Torrecuadrada JL,
654 Hoppener JW, et al. Designing antibodies for the inhibition of gastrin activity in tumoral cell
655 lines. *Int J Cancer.* 2008;122:2351-9.

656 [25] Babel I, Barderas R, Diaz-Uriarte R, Martinez-Torrecuadrada JL, Sanchez-Carbayo M,
657 Casal JI. Identification of tumor-associated autoantigens for the diagnosis of colorectal cancer in
658 serum using high density protein microarrays. *Mol Cell Proteomics.* 2009;8:2382-95.

659 [26] Babel I, Barderas R, Diaz-Uriarte R, Moreno V, Suarez A, Fernandez-Acenero MJ, et al.
660 Identification of MST1/STK4 and SULF1 proteins as autoantibody targets for the diagnosis of
661 colorectal cancer by using phage microarrays. *Mol Cell Proteomics.* 2011;10:M110 001784.

662 [27] Barderas R, Babel I, Diaz-Uriarte R, Moreno V, Suarez A, Bonilla F, et al. An optimized
663 predictor panel for colorectal cancer diagnosis based on the combination of tumor-associated
664 antigens obtained from protein and phage microarrays. *J Proteomics.* 2012;75:4647-55.

665 [28] Team RC. R: A language and environment for statistical computing. R Foundation for
666 Statistical Computing, Vienna, Austria. 2015.

667 [29] Lubin R, Schlichtholz B, Bengoufa D, Zalcman G, Tredaniel J, Hirsch A, et al. Analysis of
668 p53 antibodies in patients with various cancers define B-cell epitopes of human p53:
669 distribution on primary structure and exposure on protein surface. *Cancer Res.* 1993;53:5872-6.

670 [30] Montero-Calle A, San Segundo-Acosta P, Garranzo-Asensio M, Rabano A, Barderas R.
671 The Molecular Misreading of APP and UBB Induces a Humoral Immune Response in
672 Alzheimer's Disease Patients with Diagnostic Ability. *Mol Neurobiol.* 2019.

673 [31] Yu X, Petritis B, Duan H, Xu D, LaBaer J. Advances in cell-free protein array methods.
674 *Expert Rev Proteomics.* 2018;15:1-11.

675 [32] Cretich M, Damin F, Chiari M. Protein microarray technology: how far off is routine
676 diagnostics? *Analyst.* 2014;139:528-42.

677 [33] Atak A, Mukherjee S, Jain R, Gupta S, Singh VA, Gahoi N, et al. Protein microarray
678 applications: Autoantibody detection and posttranslational modification. *Proteomics.*
679 2016;16:2557-69.

680 [34] Duarte JG, Blackburn JM. Advances in the development of human protein microarrays.
681 *Expert Rev Proteomics.* 2017;14:627-41.

682 [35] Anderson KS, LaBaer J. The sentinel within: exploiting the immune system for cancer
683 biomarkers. *J Proteome Res.* 2005;4:1123-33.

684 [36] Gupta S, Mukherjee S, Syed P, Pandala NG, Choudhary S, Singh VA, et al. Evaluation of
685 autoantibody signatures in meningioma patients using human proteome arrays. *Oncotarget.*
686 2017;8:58443-56.

687 [37] Syed P, Gupta S, Choudhary S, Pandala NG, Atak A, Richharia A, et al. Autoantibody
688 Profiling of Glioma Serum Samples to Identify Biomarkers Using Human Proteome Arrays. *Sci*
689 *Rep.* 2015;5:13895.

690 [38] Sjoberg R, Mattsson C, Andersson E, Hellstrom C, Uhlen M, Schwenk JM, et al.
691 Exploration of high-density protein microarrays for antibody validation and autoimmunity
692 profiling. *N Biotechnol.* 2016;33:582-92.

693 [39] Jhaveri DT, Kim MS, Thompson ED, Huang L, Sharma R, Klein AP, et al. Using
694 Quantitative Seroproteomics to Identify Antibody Biomarkers in Pancreatic Cancer. *Cancer*
695 *Immunol Res.* 2016;4:225-33.

696 [40] Lin L, Zheng J, Yu Q, Chen W, Xing J, Chen C, et al. High throughput and accurate serum
697 proteome profiling by integrated sample preparation technology and single-run data independent
698 mass spectrometry analysis. *J Proteomics.* 2018;174:9-16.

699 [41] Liu XX, Ye H, Wang P, Zhang Y, Zhang JY. Identification of 1433zeta as a potential
700 biomarker in gastric cancer by proteomicsbased analysis. *Mol Med Rep.* 2017;16:7759-65.

701 [42] Rezaei M, Nikeghbalian S, Mojtahedi Z, Ghaderi A. Identification of antibody reactive
702 proteins in pancreatic cancer using 2D immunoblotting and mass spectrometry. *Oncol Rep.*
703 2018;39:2413-21.

704 [43] Garranzo-Asensio M, Guzman-Aranguez A, Poves C, Fernandez-Acenero MJ, Montero-
705 Calle A, Ceron MA, et al. The specific seroreactivity to Np73 isoforms shows higher diagnostic
706 ability in colorectal cancer patients than the canonical p73 protein. *Sci Rep.* 2019;9:13547.

707 [44] Ott C, Dorsch E, Fraunholz M, Straub S, Kozjak-Pavlovic V. Detailed analysis of the
708 human mitochondrial contact site complex indicate a hierarchy of subunits. *PLoS One.*
709 2015;10:e0120213.

710 [45] Ning L, Pan B, Zhao YP, Liao Q, Zhang TP, Chen G, et al. [Immuno-proteomic screening
711 of human pancreatic cancer associated membrane antigens for early diagnosis]. *Zhonghua Wai*
712 *Ke Za Zhi.* 2007;45:34-8.

713 [46] Cha JD, Kim HJ, Cha IH. Genetic alterations in oral squamous cell carcinoma progression
714 detected by combining array-based comparative genomic hybridization and multiplex ligation-
715 dependent probe amplification. *Oral Surg Oral Med Oral Pathol Oral Radiol Endod.*
716 2011;111:594-607.

717 [47] Huang X, Jin M, Chen YX, Wang J, Zhai K, Chang Y, et al. ERP44 inhibits human lung
718 cancer cell migration mainly via IP3R2. *Aging (Albany NY).* 2016;8:1276-86.

719 [48] Wise R, Duhachek-Muggy S, Qi Y, Zolkiewski M, Zolkiewska A. Protein disulfide
720 isomerases in the endoplasmic reticulum promote anchorage-independent growth of breast
721 cancer cells. *Breast Cancer Res Treat.* 2016;157:241-52.

722 [49] Zaghrini C, Seitz-Polski B, Justino J, Dolla G, Payre C, Jourde-Chiche N, et al. Novel
723 ELISA for thrombospondin type 1 domain-containing 7A autoantibodies in membranous
724 nephropathy. *Kidney Int.* 2019;95:666-79.

725 [50] Pedro NF, Biselli JM, Maniglia JV, Santi-Neto D, Pavarino EC, Goloni-Bertollo EM, et al.
726 Candidate Biomarkers for Oral Squamous Cell Carcinoma: Differential Expression of Oxidative
727 Stress-Related Genes. *Asian Pac J Cancer Prev.* 2018;19:1343-9.

728 [51] Privat M, Rudewicz J, Sonnier N, Tamisier C, Ponelle-Chachuat F, Bignon YJ.
729 Antioxydation And Cell Migration Genes Are Identified as Potential Therapeutic Targets in
730 Basal-Like and BRCA1 Mutated Breast Cancer Cell Lines. *Int J Med Sci.* 2018;15:46-58.

731 [52] Kim YJ, Sertamo K, Pierrard MA, Mesmin C, Kim SY, Schlessner M, et al. Verification of
732 the biomarker candidates for non-small-cell lung cancer using a targeted proteomics approach. *J*
733 *Proteome Res.* 2015;14:1412-9.

734 [53] Davaliev K, Kostovska IM, Kiprijanovska S, Markoska K, Kubelka-Sabit K, Filipovski V,
735 et al. Proteomics analysis of malignant and benign prostate tissue by 2D DIGE/MS reveals new
736 insights into proteins involved in prostate cancer. *Prostate.* 2015;75:1586-600.

737 [54] Dukel M, Streitfeld WS, Tang TC, Backman LR, Ai L, May WS, et al. The Breast Cancer
738 Tumor Suppressor TRIM29 Is Expressed via ATM-dependent Signaling in Response to
739 Hypoxia. *J Biol Chem.* 2016;291:21541-52.

740 [55] Yuan Z, Villagra A, Peng L, Coppola D, Glozak M, Sotomayor EM, et al. The ATDC
741 (TRIM29) protein binds p53 and antagonizes p53-mediated functions. *Mol Cell Biol.*
742 2010;30:3004-15.

743 [56] Glebov OK, Rodriguez LM, Soballe P, DeNobile J, Cliatt J, Nakahara K, et al. Gene
744 expression patterns distinguish colonoscopically isolated human aberrant crypt foci from normal
745 colonic mucosa. *Cancer Epidemiol Biomarkers Prev.* 2006;15:2253-62.

746 [57] Stahl PR, Hoxha E, Wiech T, Schroder C, Simon R, Stahl RA. THSD7A expression in
747 human cancer. *Genes Chromosomes Cancer.* 2017;56:314-27.

- 748 [58] Kiyamova R, Garifulin O, Gryshkova V, Kostianets O, Shyian M, Gout I, et al. Preliminary
749 study of thyroid and colon cancers-associated antigens and their cognate autoantibodies as
750 potential cancer biomarkers. *Biomarkers*. 2012;17:362-71.
- 751 [59] Garifulin OM, Kykot VO, Gridina NY, Kiyamova RG, Gout IT, Filonenko VV.
752 Application of serex-analysis for identification of human colon cancer antigens. *Exp Oncol*.
753 2015;37:173-80.
- 754 [60] Duran-Sanchon S, Moreno L, Auge JM, Serra-Burriel M, Cuatrecasas M, Moreira L, et al.
755 Identification and validation of microRNA profiles in fecal samples for detection of colorectal
756 cancer. *Gastroenterology*. 2019.

757 **Table 1**

758 Summary of the plasma samples used in the study.

Autoantigen Discovery			
	Sample number	Age (Median \pm SD in years)	Male / Female
CRC (Stage III)	3	79 \pm 5	3/0
CRC (Stage IV)	5	68 \pm 5	1/4
Control	8	41 \pm 4	3/5
Autoantigen Validation*			
	Sample number	Age (Median \pm SD in years)	Male / Female
CRC	32	69 \pm 11	15/17
Premalignant	18	59 \pm 7	12/6
Control	30	51 \pm 10	12/18

759

760 * For a full description of these samples *see* Supplementary Table S1.

761 **Table 2**

762 Identified proteins as potential autoantibody targets in CRC that appear in <10% of agarose-
 763 based immunoprecipitation registered experiments in CRAPome.

Accession	Protein Name	Number of experiments * (found/total)	Ave SC	Max SC	Ratio
P07305	H1FO	23/281	5.1	71	0.08
P52434	POLR2H	20/281	2.3	11	0.07
O95969	SCGB1D2	1/281	1	1	0.00
Q15005	SPCS2	0	1.1	2	0.00
O14880	MGST3	0	1.7	4	0.00
Q16718	NDUFA5	4/281	1.2	2	0.01
P14174	MIF	25/281	3.9	59	0.09
P49720	PSMB3	13/281	3.1	16	0.05
P61019	RAB2A	15/281	1.9	5	0.05
P52565	ARHGDI1	17/281	2.2	10	0.06
Q14019	COTL1	0	1	1	0.00
P61224	RAP1B	17/281	2.7	11	0.06
P37837	TALDO1	10/281	2.7	13	0.04
O75489	NDUFS3	1/281	2.3	9	0.00
P00403	MT-CO2	2/281	2.7	14	0.01
P30740	SERPINB1	0/281	1	1	0.00
P04637	TP53	25/281	5.4	31	0.09
Q9NX63	CHCHD3	3/281	4.6	31	0.01
Q9BS26	ERP44	0/281	1.3	2	0.00
P61158	ACTR3	10/281	3.1	17	0.04
O43464	HTRA2	1/281	1.5	2	0.00
Q9UBU8	MORF4L1	1/281	1.5	2	0.00
Q02790	FKBP4	28/281	6.7	52	0.10
Q9UPZ6	THSD7A	0	1	1	0.00
P35228	NOS2	1/281	1	1	0.00
Q8N3J5	PPM1K	4/281	2	2	0.01
Q14134	TRIM29	1/281	1.2	2	0.00
Q9P2B4	CTTNBP2NL	1/281	1	1	0.00
P33992	MCM5	22/281	5	34	0.08
Q92794	KAT6A	0	2	2	0.00
Q9HD67	MYO10	0	1	1	0.00

764 * Agarose beads immunoprecipitations. Proteins highlighted in grey were used for
 765 validation.

766 **Legend to the Figures**

767

768 **Fig. 1.** Schematic work-flow of the modified SASI approach used for the identification and
769 validation of CRC autoantigens. Immunoprecipitation coupled to mass spectrometry of a CRC
770 cell protein extract using isolated IgGs from plasma samples was used to identify tumor-
771 associated antigens target of CRC autoantibodies. The identified potential targets were analyzed
772 using bioinformatics tools and validated through different techniques. Arrows depicted in the
773 SDS-PAGE highlight those protein bands that seem to differ between the immunoprecipitation
774 using control IgGs and CRC IgGs.

775

776 **Fig. 2.** Bioinformatics analysis of the autoantibody targets. (A) cBioPortal data on CRC showed
777 that 69% and 80% of the identified targets had genetic alterations in tissue samples from colon
778 and rectal adenocarcinomas, respectively. (B) The Oncomine and UALCAN databases showed
779 that 22 out of the 31 identified proteins had a statistically significant altered expression ($p < 0.05$)
780 in CRC in comparison to adjacent paired healthy tissue. (C) The Human Protein Atlas [18, 19]
781 showed that CTTNBP2NL has been described as a CRC prognosis marker.

782

783 **Fig. 3.** The identified targets of CRC autoantibodies are dysregulated at protein level in tissue
784 samples. (A) IHC analysis showed that indicated proteins were present in colorectal
785 pathological tissue. (B) TALDO1 and ERP44 could significantly discriminate between stage II
786 CRC patients (p -value < 0.05). (C) ROC curves analysis of the IHC data showed that ERP44 had
787 an AUC of 70% (40% sensitivity, 100% specificity) to discriminate CRC patients according to
788 survival status. TALDO1 showed an AUC of 63.4% (56.9% sensitivity, 66.7% specificity)
789 when grouping patients according to recurrence status. When grouping patients according to
790 disease free survival, the AUC of ERP44 was 61.4% (59.1% sensitivity, and 65.9% specificity).

791

792 **Fig. 4.** Cloning, *in vitro* protein expression and evaluation of seroreactivity levels of 13
793 potential autoantibody targets of CRC autoantibodies. (A) Confirmation of the *in vitro* protein

794 expression of the 13 selected targets as HaloTag fusion proteins. (B) Seroreactivity levels of the
795 13 proteins using the indicated 80 individual plasma samples (Table 1; Supplementary Table
796 S1). (C) Autoantibody levels against CHCHD3 (p-value = 4.57e-05), CTTNBP2NL (p-value =
797 0.00074), FKBP4 (p-value = 0.00079), MGST3 (p-value = 4.36e-05), THSD7A (p-value =
798 9.23e-05), and TRIM29 (p-value = 0.0027) as well as p53 (p-value = 0.011) could discriminate
799 with statistical significance between the asymptomatic healthy control group and the CRC
800 group. (D) Autoantibody levels of CTTNBP2NL (p-value = 0.00028), FKBP4 (p-value =
801 0.0014), and TALDO1 (p-value = 0.010) were able to significantly discriminate between
802 asymptomatic healthy control individuals and premalignant subjects. (E) Autoantibody levels
803 against ERP44 (p-value = 0.045), TALDO1 (p-value = 0.018), CHCHD3 (p-value = 0.0024),
804 CTTNBP2NL (p-value = 6.68e-05), FKBP4 (p-value = 0.00015), MGST3 (p-value = 0.002),
805 THSD7A (p-value = 0.014), and TRIM29 (p-value = 0.0045)-as well as p53 (p-value = 0.041)
806 were able to discriminate between the asymptomatic healthy control individuals and the
807 colorectal pathological group.

808

809 **Fig. 5.** Evaluation of the diagnostic value of CRC autoantibodies. (A) The combination of
810 CHCHD3, CTTNBP2NL, FKBP4, MGST3, THSD7A, and TRIM29 showed an AUC of 99.7%,
811 with a sensitivity of 96.9% and specificity of 100%. (B) Autoantibodies against CTTNBP2NL,
812 FKBP4, and TALDO1 showed an AUC of 88.9% with a sensitivity of 83.3% and specificity of
813 86.7% when discriminating asymptomatic healthy control individuals and premalignant
814 subjects. (C) Combined detection of autoantibodies against CHCHD3, CTTNBP2NL, ERP44,
815 FKBP4, MGST3, TALDO1, THSD7A, TRIM29, and p53 showed an AUC of 95.3%, with a
816 sensitivity of 92.0% and a specificity of 90.0% when discriminating the asymptomatic healthy
817 control individuals and the pathological group.

818 **Legend to the Supplementary Figures**

819

820 **Supplementary Fig. 1.** Bioinformatic analysis of the identified targets by STRING and IPA.

821 (A) Clustering of the direct and indirect interactions of the identified autoantibody targets
822 performed with STRING. Direct and indirect clustering of proteins showed five interacting
823 groups composed of proteins related to GTPases and actin-interacting proteins, transcription,
824 immunity, and cell cycle functions; pentose pathways and endoplasmic reticulum, respiratory
825 chain and caspase activity, and respiratory chain and cell messengers. (B) IPA analysis of the
826 identified targets. Among the identified altered networks appeared the cell cycle, DNA
827 replication, recombination, protein synthesis; and cancer, carbohydrate metabolism, and cell
828 cycle networks.

829

830 **Supplementary Fig. 2.** Verification of the presence of the autoantibody targets at mRNA and

831 protein level in the CRC cells used in the study. (A) mRNA level. (B) Protein level. GAPDH
832 and tubulin were used as loading controls at mRNA and protein level, respectively.

Figure 1

[Click here to download high resolution image](#)

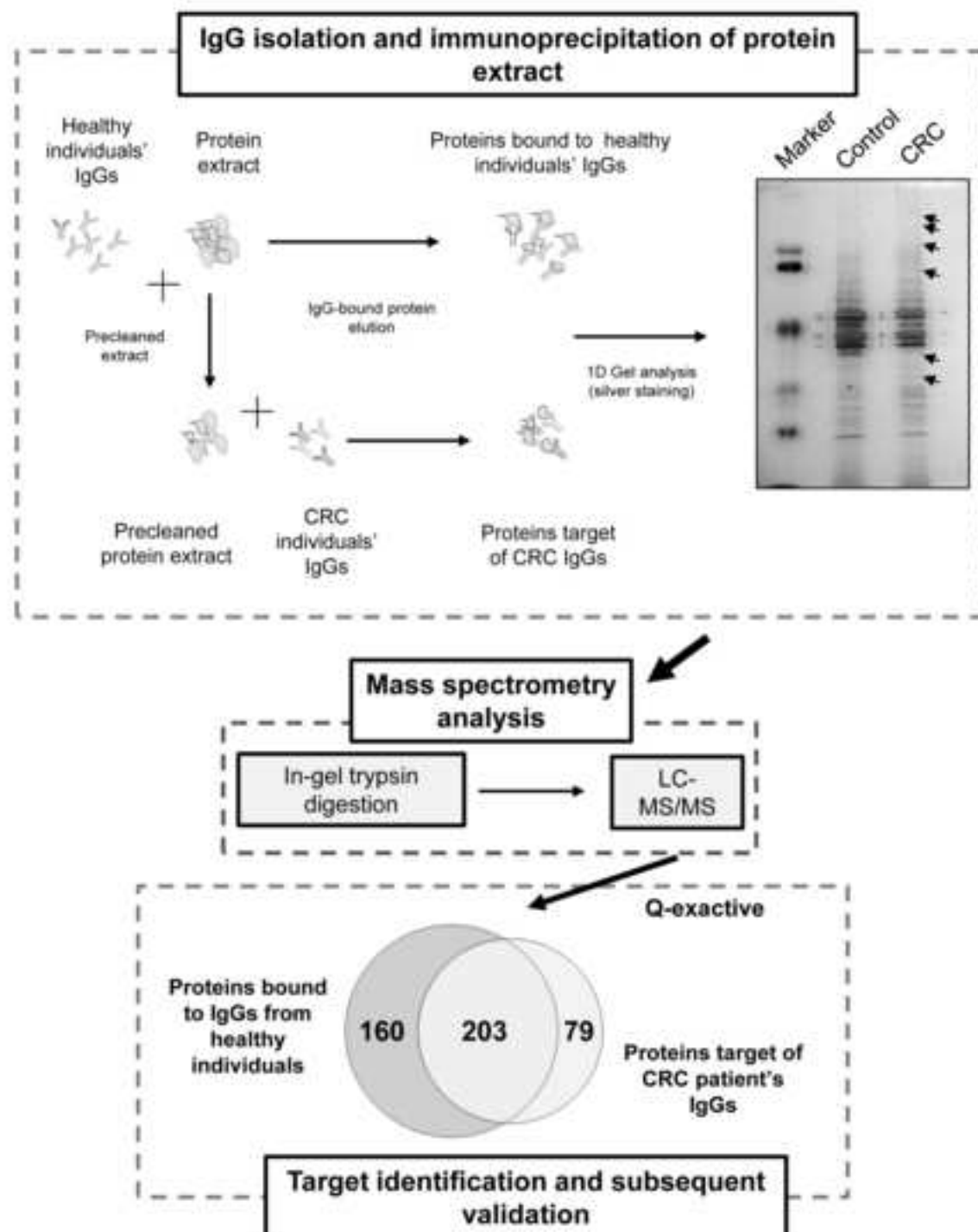


Figure 1

Figure 2
[Click here to download high resolution image](#)

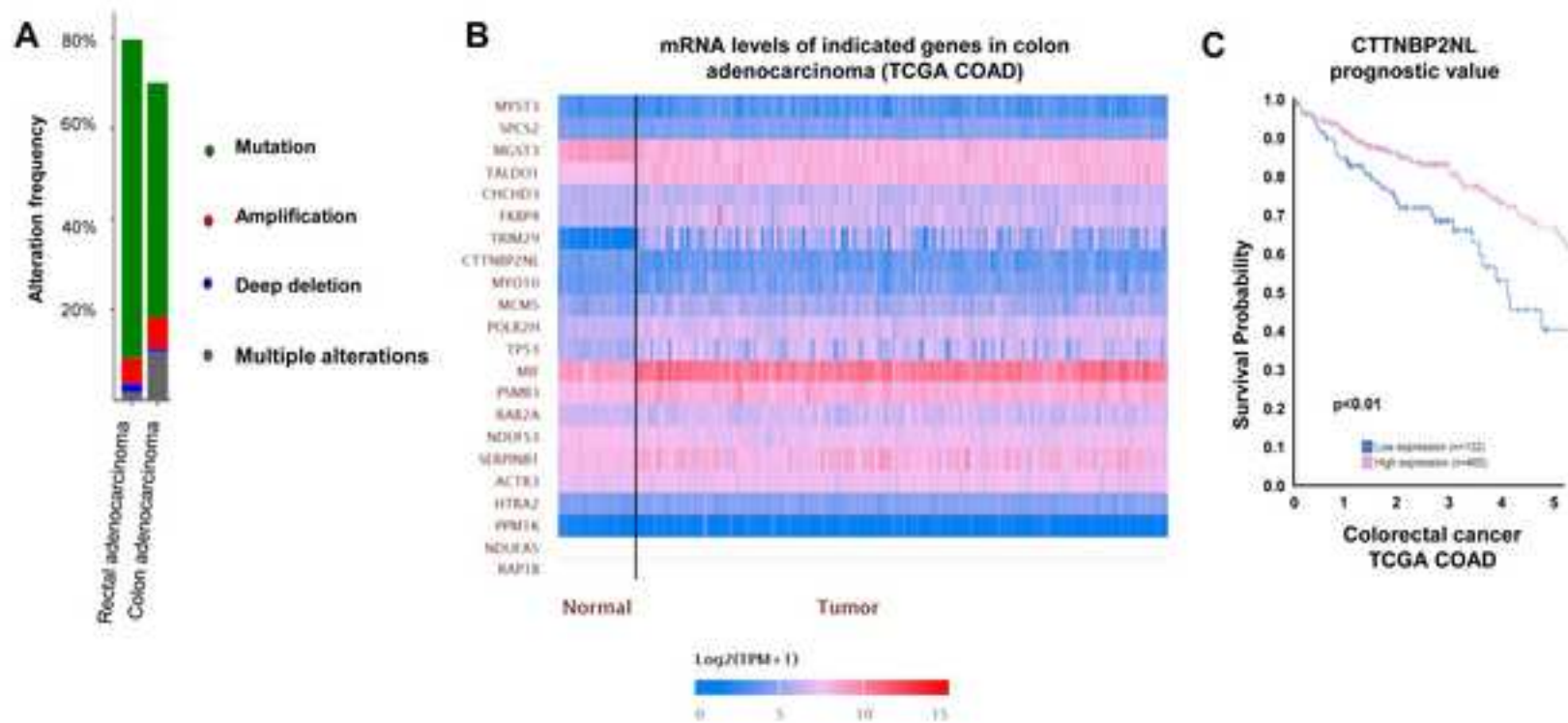


Figure 2

Figure 3
[Click here to download high resolution image](#)

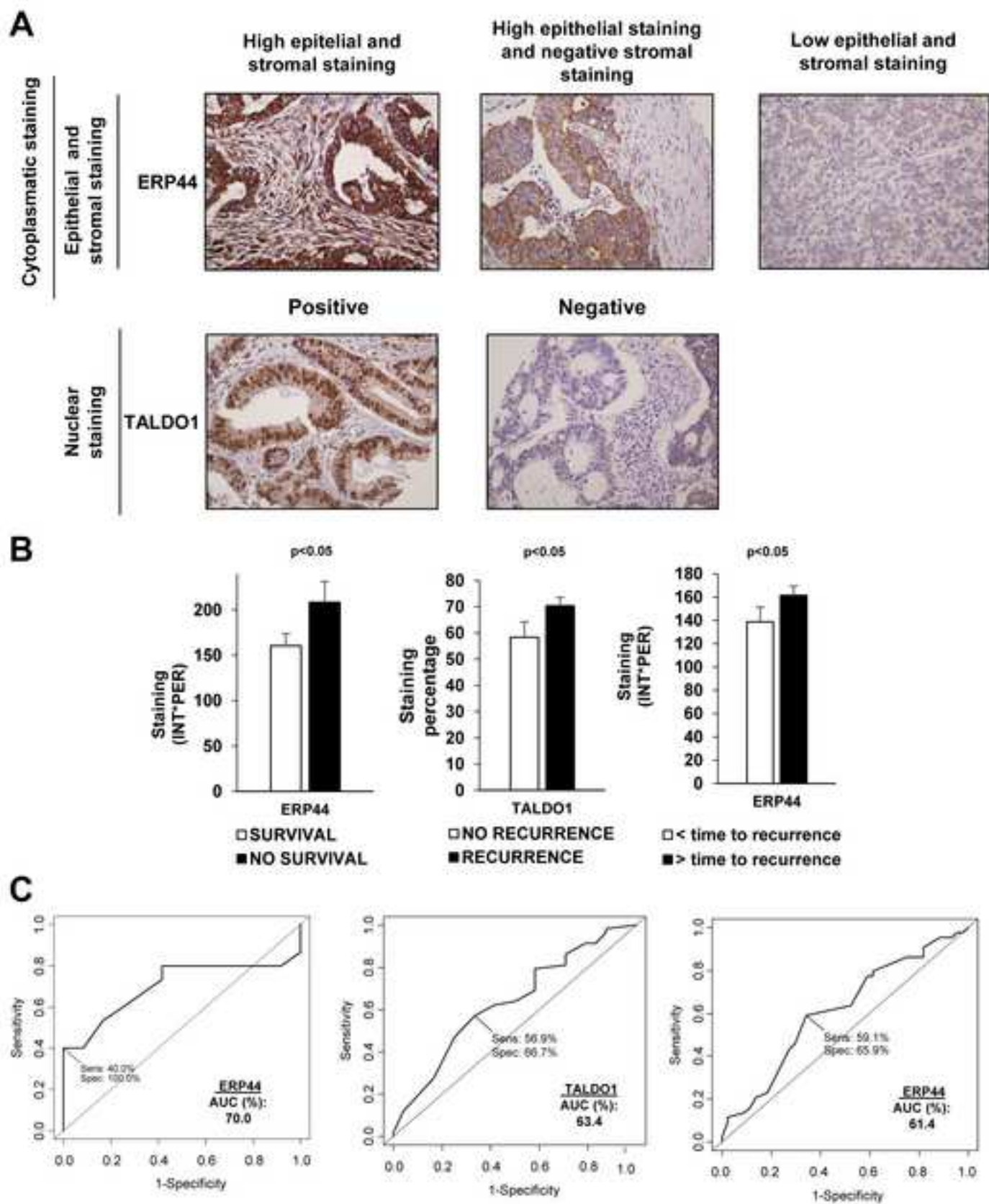


Figure 3

Figure 4
[Click here to download high resolution image](#)

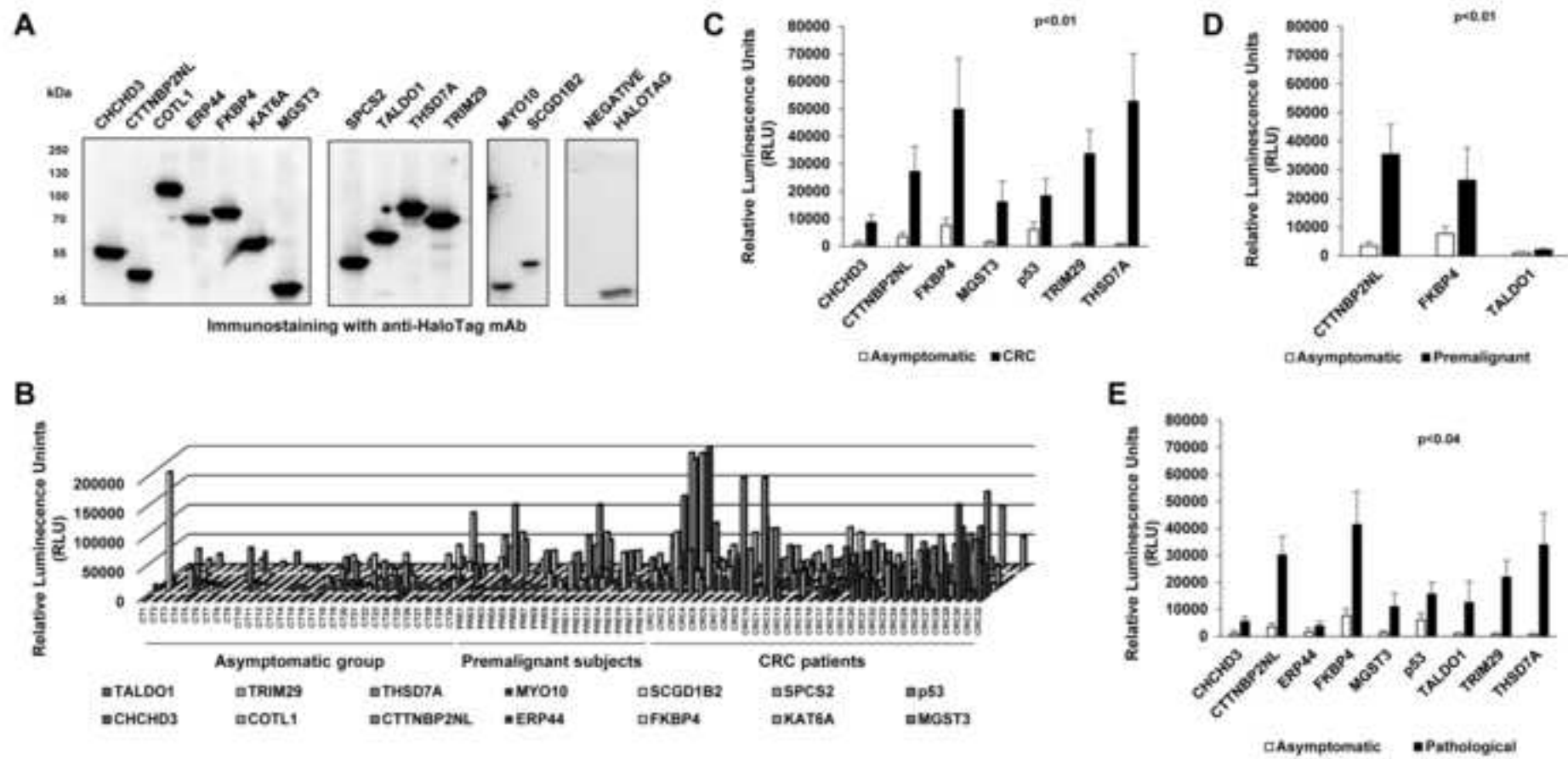


Figure 4

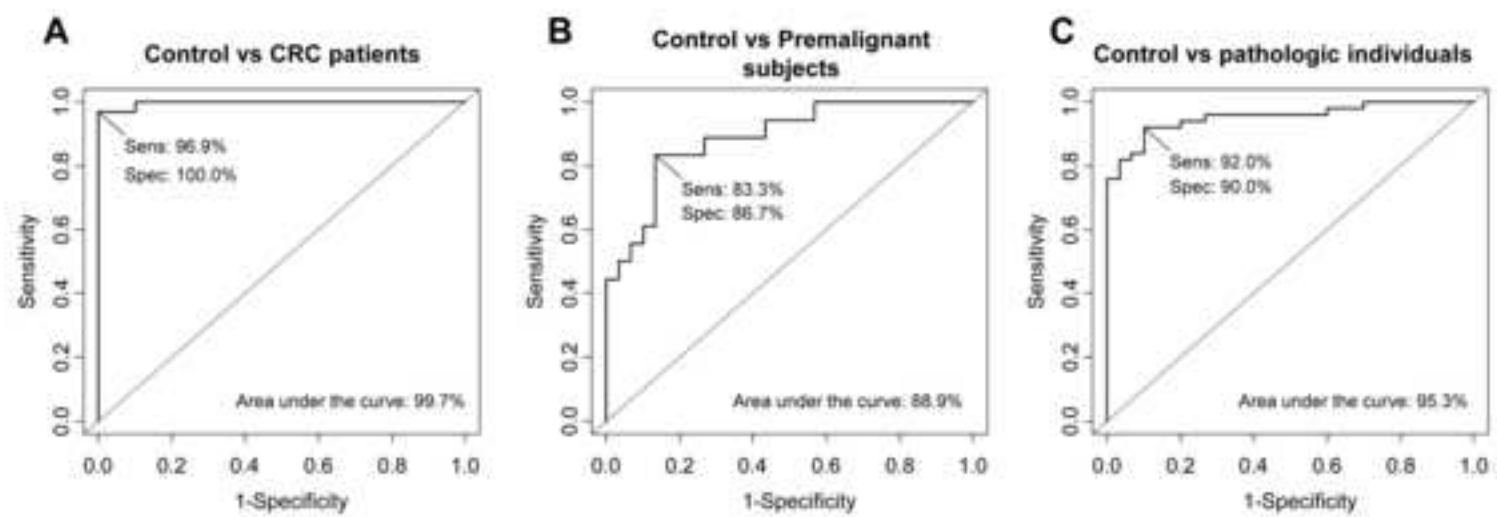


Figure 5

Supplementary Fig S1

[Click here to download Supplementary material: Supplementary Fig. S1.tif](#)

Supplementary Fig S2

[Click here to download Supplementary material: Supplementary Fig. S2.tiff](#)

Supplementary Table S1

[Click here to download Supplementary material: Supplementary Table S1.xlsx](#)

Supplementary Table S2

[Click here to download Supplementary material: Supplementary Table S2.xlsx](#)

Supplementary Table S3

[Click here to download Supplementary material: Supplementary Table S3.xlsx](#)

Supplementary Table S4

[Click here to download Supplementary material: Supplementary Table S4.xlsx](#)

Supplementary Table S5

[Click here to download Supplementary material: Supplementary Table S5.xlsx](#)

Supplementary Table S6

[Click here to download Supplementary material: Supplementary Table S6.xlsx](#)

***Conflict of Interest**

[Click here to download Conflict of Interest: coi_disclosure All Authors.pdf](#)